Paper n. 089

STABILITY ANALYSIS OF HELICOPTER ROTORS IN FORWARD FLIGHT VIA STATE-SPACE AEROELASTIC MODELING AND CORRELATION WITH EXPERIMENTAL RESULTS

D. Muro and M. Gennaretti

University Roma Tre
Dept. of Mechanical and Industrial Engineering
Via della Vasca Navale 79 - 00146 Rome, Italy
e-mail: d.muro@uniroma3.it

Abstract

Reduced-order aerodynamic models are tools that may be conveniently applied in a wide range of research and design applications in the aeronautical and mechanical fields. This paper presents aeroelastic applications of a Reduced-Order Model suited for the description of the linearized unsteady aerodynamics of helicopter rotors in arbitrary steady flight. It is defined in terms of multiblade coordinates and allows the derivation of state-space aeroelastic operators that are useful for stability analysis and aeroservoelastic applications. An aerodynamic solver has to be applied to get a set of harmonic responses from which the aerodynamic ROM is identified. In this paper, the state-space aeroelastic model of a four bladed hingeless soft-inplane helicopter main rotor in forward flight is derived, through harmonic solutions predicted by a potential-flow Boundary Element Method solver. It is applied to the analysis of the aeroelastic stability in several flight conditions, and the corresponding results are compared with experimental and numerical data available in the literature. These correlations validate the proposed procedure as suitable for the identification of state-space rotor aeroelastic models.

List of Symbols

A_i	= amplitude of i-th multiblade force
$\mathbf{A}$	=multiblade state-space constant matrix
$\mathbf{A}_i, \mathbf{G}, \mathbf{H}, \mathbf{R}$	=matrices of the rational approximation
C_T	= thrust coefficient
$\mathbf{E}$	=aerodynamic matrix
$\mathbf{f}^M$	=vector of multiblade aerodynamic forces
G	=unit source solution
M_j	= amplitude of j-th multiblade coordinate
$\mathbf{r}$	=additional multiblade aerodynamic states
t	=time
$\mathbf{x}$	=observer position
$\mathbf{x}^M$	=multiblade coordinates
$\mathbf{y}$	=source position
$\mathbf{z}$	=aeroelastic multiblade state variables
θ_i	= phase of i-th multiblade force
$\theta_0, \theta_c, \theta_s$	= pitch control settings
μ	= advance ratio
φ	=velocity potential
ω	=angular frequency

Introduction

The aim of this work is the application of the aerodynamic Reduced-Order Model (ROM) presented in Ref. [1] for the aeroelastic stability analysis of a hingeless helicopter rotor in forward flight. From the proposed reduced-order aerodynamic modeling, the formulation of rotor aeroelastic problems in state-space form may be obtained. It is particularly convenient for the stability analysis, in that allows the eigenanalysis and hence the evaluation of aeroelastic dampings and frequencies. Furthermore, it is an important tool for aeroservoelastic applications aimed at the design of controllers for stability augmentation and alleviation of responses to external perturbations (*e.g.,* atmospheric gusts).

In the past, reduced-order models for the aerodynamic loads arising on helicopter rotors have been developed by Peters and his co-workers (see for instance, Refs. [2, 3, 4]). These are based on the finite-state approximation of the wake inflow and have inspired the work of many of the researchers interested in rotor aeroelastic analyses. In these formulations the aerodynamic loads are obtained coupling blade sectional load models with wake vorticity effects and are strongly dependent on the

wake shape. Several formulations of different complexity have been developed in the last years, taking into account wake distortion effects (see, for instance, [5] and [6]).

The approach introduced in Ref. [1] yields the identification of a linear aerodynamic ROM for the perturbation analysis of helicopter rotors in forward flight, defined in terms of multiblade coordinates. It is based on rotor harmonic responses obtained through a time-marching aerodynamic solver, and the ROM derived is a constant-coefficient differential model relating multiblade rotor coordinates to the generalized aerodynamic forces in the multiblade frame [1]. The expression of the ROM is the result of the rational approximation of the matrix collecting the multiblade transfer functions determined through the harmonic responses [7]. From this point of view, the proposed method is inspired to the fixed-wing, finite-state formulations investigated by Vepa [8], Edwards [9], Roger [10], and particularly to that applied by Karpel [11]. It is worth pointing out that the accuracy of the identified aerodynamic ROM depends on the accuracy of the aerodynamic solver applied for the harmonic responses and, if allowed by the solver capabilities, may take into account complex aerodynamic effects with inclusion of wake roll-up and blade-vortex interactions.

Here, the aerodynamic ROM for the hingeless, four-bladed helicopter main rotor examined in Refs. [12, 13] is identified, starting from the aerodynamic harmonic responses predicted by a potential-flow, Boundary Element Method (BEM) solver. The helicopter rotor state-space aeroelastic model is obtained by coupling the aerodynamic ROM with a flap-lag-torsion structural dynamics model derived from the differential equations in Ref. [14], through application of the Galerkin approach [15]. Then, the rotor frequencies and dampings are evaluated by the eigenanalysis of the aeroelastic operator. In order to assess the accuracy and reliability of the proposed approach for the stability analysis of a realistic helicopter rotor configuration, these results are compared with experimental and numerical data available in the literature [12, 13], and the corresponding correlations are presented and discussed in the Numerical Results section.

Procedure for identification of ROM

In this Section an outline of the aerodynamic ROM identification procedure for rotors introduced in Ref. [1] is provided.

The state-space, perturbation aeroelastic modeling of helicopter rotors in forward flight is mathematically described by means of periodic-coefficient differential equations. Mainly, this is due to the periodicity of the blade relative wind, the cyclic pitch control and the rotor-disk inflow distribution generated by the wake vorticity [16, 17]. These equations may be applied for the linearized stability analysis around a periodic equilibrium condition and the aeroelastic spectrum may be evaluated exactly by means of the Floquet theory. However, the application of this theory (or the improved Fast-Floquet and Generalized-Fast-Floquet theories [18]) requires the evaluation of a number of responses to state perturbations that may be computationally expensive and, further, the interpretation of the frequencies and eigenmodes is a difficult task [16, 17]. For this reason, the application of the multiblade coordinates transformation [16], followed by the constant-coefficient approximation of the corresponding aeroelastic equations has been successfully introduced in the past for flight configurations with low and low-mid advance ratios (approximately, for $\mu < 0.3$) [17]. In this form, the representation of the rotor aeroelastic behavior is well suited for standard eigenanalysis and for aeroservoelastic applications. As a consequence, this approach is widely used for helicopter rotor aeroelastic analysis (especially in the context of multidisciplinary optimization processes and preliminary design).

The effectiveness of the constant-coefficient approximation of the aeroelastic system written in multiblade coordinates has inspired the aerodynamic ROM presented in Ref. [1]. It yields the multiblade aerodynamic loads as explicit, constant-coefficient, differential forms of the multiblade coordinates, through the following three-step identification procedure:

Evaluation of multiblade frequency response functions

This is the key point of the procedure, which is inspired by the fact that the state-space relationship between perturbation multiblade coordinates and multiblade loads, under constant-coefficient approximation, is a constant-coefficient, linear, differential form. In the frequency-domain, it is represented by a transfer function that, at a given frequency, may be identified from the frequency response through amplitude and phase of the output with respect to those of the (same frequency) input (indeed, single-harmonic inputs yield multi-harmonic outputs only in periodic-coefficient and/or nonlinear differential forms). The evaluation of the multiblade frequency response functions is obtained as follows: (i) a time marching aerodynamic solver is applied to evaluate the (generalized) multiblade aerodynamic loads due to single-harmonic small oscillations of each multiblade coordinate; (ii) the contributions having the same harmonic of the input are extracted from the responses; (iii) the corresponding frequency-response complex values are determined, and (iv) the process is repeated for a discrete number of frequencies within an appropriate range, so as to get an adequate sampling of the frequency-response functions.
Hence, as required, the procedure applied is such that only the constant-coefficient, linear(ized), portions of the differential form relating perturbation multiblade coordinates and multiblade loads are retained.

Rational matrix approximation

The frequency-response functions evaluated from the harmonic responses are collected into an aerodynamic matrix, $\mathbf{E}(s)$, which in turn is approximated in rational form. Specifically, the aerodynamic matrix, $\mathbf{E}(s)$, relating the vector of the frequency-domain multiblade coordinates, $\tilde{\mathbf{x}}^M$, to the vector of the frequency-domai nmultiblade aerodynamic loads, $\tilde{\mathbf{f}}^M$, is approximated as

$$\mathbf{E}(s) \approx s^2\,\mathbf{A}_2 + s\,\mathbf{A}_1 + \mathbf{A}_0 + \mathbf{H}\left[s\,\mathbf{I} - \mathbf{G}\right]^{-1}\,\mathbf{R} \qquad (1)$$

through a least-square procedure assuring that the identified complex poles have (stable) negative real parts. Matrices $\mathbf{A}_2, \mathbf{A}_1, \mathbf{A}_0, \mathbf{G}, \mathbf{H}$ and $\mathbf{R}$ are real, fully populated matrices. The inclusion of the rational contributions is suggested by the shapes of the frequency-response functions evaluated, which are not expected to be well approximated by polynomial forms due to the influence of the wake unsteady vorticity (theoretical models show that it is responsible for the transcendental terms appearing in the sectional aerodynamics transfer functions [19, 20, 7]).

Identification of the differential model

Transforming back into time domain the approximated rational expressions identified above, the aerodynamic ROM is obtained in terms of the following differential form relating multiblade coordinates to multiblade aerodynamic loads

$$\begin{aligned} \mathbf{f}^M(t) &= \mathbf{A}_2\ddot{\mathbf{x}}^M + \mathbf{A}_1\dot{\mathbf{x}}^M + \mathbf{A}_0\mathbf{x}^M + \mathbf{H}\mathbf{r} \\ \dot{\mathbf{r}} &= \mathbf{G}\mathbf{r} + \mathbf{R}\mathbf{x}^M \end{aligned} \tag{2}$$

where $\mathbf{r}$ is the vector of the additional aerodynamic states (in the multiblade-variable space, under constant-coefficient approximation) associated to the poles of the rational approximation. Note that the accuracy of the final identified ROM in predicting perturbation aerodynamic loads depends on the accuracy of the aerodynamic solver applied to evaluate the harmonic responses.

Remarks on the numerical identification of frequency response functions

In the identification procedure of the transfer functions, some crucial issues have to be taken into consideration, in order to avoid inaccuracies or mistakes.

For a given j-th perturbation harmonic multiblade coordinate input of frequency ω_k about a given periodic equilibrium motion

$$x_j^M = M_j \cos(\omega_k t) \tag{3}$$

with small amplitude, M_j, the aerodynamic solver computes the corresponding multiblade aerodynamic loads. Then, for A_i and θ_i denoting, respectively, amplitude and phase of the ω_k-harmonic component of the multiblade response f_i^M, the corresponding frequency response function, $E_{ij}(\omega_k)$, is determined as

$$\begin{aligned} Re[E_{ij}(\omega_k)] &= (A_i/M_j)\cos(\theta_i) \\ Im[E_{ij}(\omega_k)] &= (A_i/M_j)\sin(\theta_i) \end{aligned}$$

Note that extracting from the perturbation output only the contribution having the same harmonic of the input implies that, as mentioned above, a linearized, constant-coefficient approximation of the relation between perturbation multiblade quantities is pursued (indeed, in nonlinear and/or periodic-coefficient relations a single-harmonic input yields multi-harmonic outputs).

The harmonic components are obtained through a Fast Fourier Transform (FFT) algorithm, taking care of the following issues: (i) the period examined by the FFT starts after that the rotor wake is fully developed (and transient response is finished); (ii) in order to avoid leakage effects, the period examined has to be an integer multiple of the period of the input harmonic; (iii) almost periodic loads might arise because of the intrinsic periodicity of the aerodynamic system, and hence the leakage avoidance is assured if, in addition, the period examined is wide enough (a numerical convergence analysis has shown that the length of the period examined equal to thirty periods of the input harmonic is suitable for the problem analyzed in this work); (iv) the time interval of the time marching solution is chosen so as to have an integer number of time steps falling into the examination period.

Remarks on rational matrix approximation

In expressing the aerodynamic matrix in rational form the identification of the poles is a key point. Indeed, more sets of poles could provide mathematically equivalent rational approximations of the aerodynamic matrix, and an inappropriate choice of the one to be applied could invalidate the realistic simulation of the aeroelastic system. In particular, realistic aerodynamic poles have to be stable with suited margin of stability, and this constraint has to be included in the least-square approximation procedure. Unstable poles would clearly represent an unrealistic aerodynamic behavior (an impulsive blade motion would generate indefinitely growing aerodynamic loads), but the same would occur for poles close to the imaginary axis, in that making aerodynamics prone to resonance. This problem is illustrated in Figs. 1 and 2 that present the aeroelastic eigenvalues derived from the proposed approach for two different sets of aerodynamic poles (yielding very similar rational matrix approximations), concerning a four-bladed, hinged, flap-lag rotor in forward flight at $\mu = 0.16$. Specifically, Fig. 1 shows that the rational approximation with a subset of aerodynamic poles lying on the imaginary axis yields an aeroelastic spectrum with some of the aerodynamic eigenvalues (*i.e.,* associated to aerodynamic eigenvectors) that are unstable, while Fig. 2 demonstrates that imposing a margin of stability to the poles of the rational form, the corresponding aerodynamic eigenvalues are all stable. Furthermore, comparing Figs. 1 and 2 shows that the (critical) structural eigenvalues are barely affected by the stability margin of the poles of the rational form, and are stable in both cases. Therefore, having a set of poles too close to the imaginary axis may be misleading in terms of interpretation of the aeroelastic stability of the system, while making the resulting aeroelastic state-space representation unsuitable for time-marching predictions and/or aeroservoelastic applications.

The aerodynamic solver

In this work, the aerodynamic solver applied to compute the harmonic responses required in the ROM identification procedure is based on the BEM formulation for potential flows presented in Ref. [21].

For φ denoting the velocity potential function (*i.e.,* such that the velocity field is given by $\mathbf{v} = \nabla\varphi$), this BEM formulation stems from the potential-field solution for

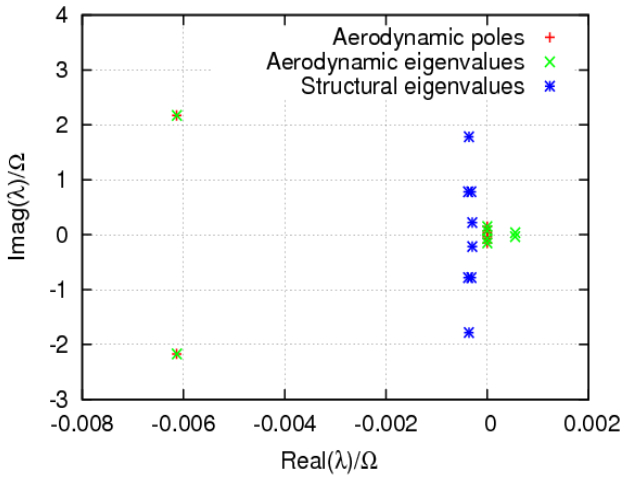

Figure 1. Aeroelastic eigenvalues due to inappropriate poles placement.

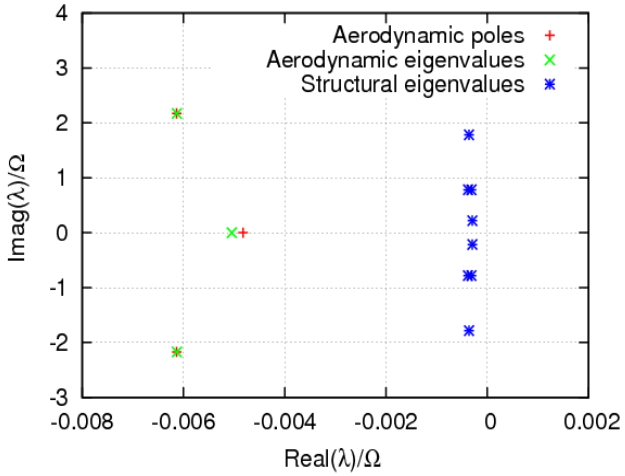

Figure 2. Aeroelastic eigenvalues due to appropriate poles placement.

the arbitrary motion of a lifting body obtained through the following boundary integral representation

$$\begin{aligned}\varphi(\mathbf{x},t) &= \int_{\mathcal{S}_B}\left(\frac{\partial\varphi}{\partial n}\,G-\varphi\,\frac{\partial G}{\partial n}\right)\mathrm{d}\mathcal{S}(\mathbf{y})\\ &- \int_{\mathcal{S}_W}\Delta\varphi(\mathbf{x}_{TE},t-\tau)\,\frac{\partial G}{\partial n}\,\mathrm{d}\mathcal{S}(\mathbf{y}) \qquad (4)\end{aligned}$$

where $\mathcal{S}_B$ denotes the body surface, and $\mathcal{S}_W$ denotes the zero-thickness wake surface where the vorticity generated by the body remains confined. In addition, $G=-1/4\pi\|\mathbf{x}-\mathbf{y}\|$ is the fundamental solution of the Laplace equation, $\partial/\partial n=\mathbf{n}\cdot\nabla$ with $\mathbf{n}$ denotes the outward unit normal to the body surface, whereas $\Delta\varphi(\mathbf{x}_{TE},t-\tau)$ is the potential discontinuity at the trailing edge location where the wake point was released at the delayed time $t-\tau$. Furthermore, the application of the body surface impermeability condition yields the boundary condition, $\partial\varphi/\partial n=\mathbf{v}_B\cdot\mathbf{n}$, where $\mathbf{v}_B$ denotes the velocity of the body surface points. For $\mathbf{x}$ approaching $\mathcal{S}_B$, Eq. (4) yields an integral equation which may be used to obtain the values of φ on $\mathcal{S}_B$ [21]. Equation (4) is solved numerically by boundary elements, *i.e.,* by the discretization of $\mathcal{S}_B$ and $\mathcal{S}_W$ into quadrilateral panels, assuming φ, $\partial\varphi/\partial n$ and $\Delta\varphi$ to be piecewise constant (zero-th order BEM), and imposing that the equation be satisfied at the center of each body element (collocation method).

Once the potential on the body surface has been determined, the Bernoulli theorem yields the pressure distribution, and hence the aerodynamic forces acting on it may be evaluated. This aerodynamic formulation may be applied both with prescribed wake shapes and for deforming free-wake analysis. In the free-wake approach, the shape of the wake is obtained as part of the solution. Indeed, once φ on the surface is known, the application of the gradient operator to Eq. (4) yields an integral representation of the velocity field. Thus, at each step of the time-marching procedure, the wake points are moved accordingly to the local velocity field and the shape of the wake is continuously renewed.

For the evaluation of the multiblade-space harmonic responses to be processed in the ROM identification procedure, first the rotating blade coordinates are derived from the harmonic input multiblade coordinate, then the aerodynamic solver yields the corresponding generalized aerodynamic forces in the rotating frame, and finally the multiblade generalized loads are determined by application of the multiblade transformation.

Numerical results

In order to assess the accuracy and reliability of the finite-state aeroelastic modelling derived by combining the presented ROM procedure with the BEM aerodynamic solver outlined above, the stability of a realistic helicopter rotor configuration in forward flight is examined. Note that the accuracy of the ROM aerodynamic approach in rotor aeroelastic applications has been widely discussed in Ref. [1], for advance ratios included in the range $0\leq\mu\leq 0.26$. The numerical applications concern the soft-inplane, hingeless, four-bladed rotor with torsionally soft blades, that has been experimentally investigated at the AFDD [12]. The untwisted blades have length $R=1.143$m, NACA 0012 airfol sections, chord $c=0.08636$m, and precone angle equal to 2° (a detailed description of the structural properties are available in Refs. [13, 12]). A critical structural damping of 1% is included in the analysis, according to the measured structural damping [12].

In this work, the rotor blade structural dynamics is described through a beam-like model. It is based on the nonlinear bending-torsion equations of motion presented in Ref. [14], that are valid for straight, slender, homogeneous, isotropic, nonuniform, twisted blades. Retaining second order terms after the application of an ordering scheme that drops third-order terms not contributing to damping, and assuming radial displacements as simply geometric consequences of the transverse bending deflections [22], the final form of the dynamic system is a set of coupled nonlinear integro-partial differential equations having as unknowns in-plane and out-of-plane displacements of the elastic axis, along with the cross-section elastic torsion. It is suitable for describing the response of beam-like structures undergoing significant deflections. The space discretization of the equations is performed through the Galerkin method, based on elastic deformations described as a linear combination

	Present data	Ref. [12]
[1mm] 1*st* flap	0.16/*rev*	0.15/*rev*
2*nd* flap	1.01/*rev*	1.0/*rev*
1*st* lag	0.507/*rev*	0.5/*rev*
1*st* torsion	2.2/*rev*	2.3/*rev*

Table 1. Nonrotating vibration natural frequencies.

	Present data	Ref. [12]
[1mm] 1*st* flap	1.15/*rev*	1.13/*rev*
2*nd* flap	2.92/*rev*	2.9/*rev*
1*st* lag	0.71/*rev*	0.71/*rev*
1*st* torsion	2.42/*rev*	2.56/*rev*

Table 2. Rotating vibration natural frequencies.

of suitable linearly independent shape functions that satisfy the geometric homogeneous boundary conditions corresponding to the structure constraints; in our problem dealing with hingeless blades they are chosen as the bending natural modes of a cantilever beam [15]. Applying the constant-coefficient multiblade transformation to resulting ordinary differential equations linearized about a given equilibrium state, and coupling them with Eq. (2) (where the generalized forces are those obtained from projection of the sectional aerodynamic loads onto the shape functions used in the Galerkin approach) yields the following perturbation state-space aeroelastic representation

$$\dot{\mathbf{z}} = \mathbf{A}\,\mathbf{z} \tag{5}$$

where $\mathbf{z}$ is the vector of the multiblade state variables (structural coordinates plus additional aerodynamic states), while $\mathbf{A}$ is the constant aeroelastic state matrix.

First, the structural dynamics solver is applied to assess the number of shape functions to be used in the aeroelastic analysis. To this aim, the nonrotating and rotating natural frequencies of vibration evaluated by the numerical solver mentioned above are compared with those presented in Ref. [12] (with the rotating ones related to the nominal rotor speed). Tables 1 and 2 show the comparison between the two set of data, with the present numerical prediction carried out using four in-plane bending modes, two out-of-plane bending modes and one torsion mode (note that nonrotating frequencies from Ref. [12] have to be considered affected by a slight uncertainty in that derived from a fan plot). Because of the satisfactory agreement observed in these tables, all the aeroelastic results that will be presented in the following have been obtained through this set of shape functions.

The rotor aeroelastic stability analysis has been performed for $0.04 \leq \mu \leq 0.2537$, considering the trim data condition presented in Ref. [13] and given in Table 3. The equilibrium deformation of the rotor has been obtained using in the aeroelastic solver a quasi-steady aerodynamic model with Drees static inflow (this implies that the aerodynamic solver used in ROM procedure is different from that used in the identification of the steady-state equilibrium configuration).

μ	θ_0	θ_c	θ_s	C_T
0.04	5.86	1.495	−1.359	0.00376
0.1	5.72	1.154	−1.942	0.00429
0.2028	5.94	0.195	−3.491	0.00339
0.2537	5.95	0.081	−3.79	0.00252

Table 3. Rotor trim data.

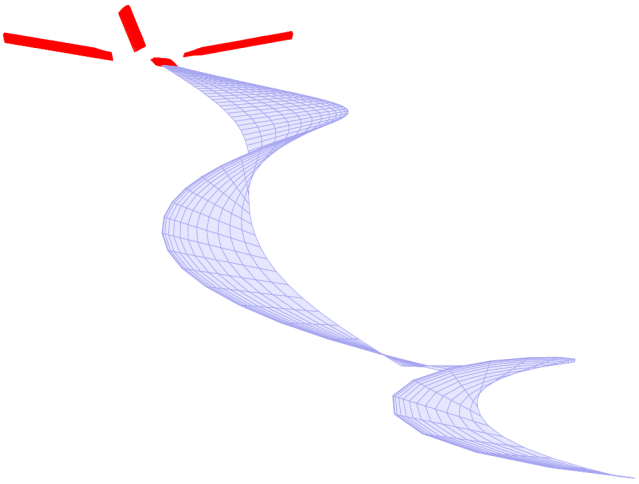

Figure 3. Undeformed wake

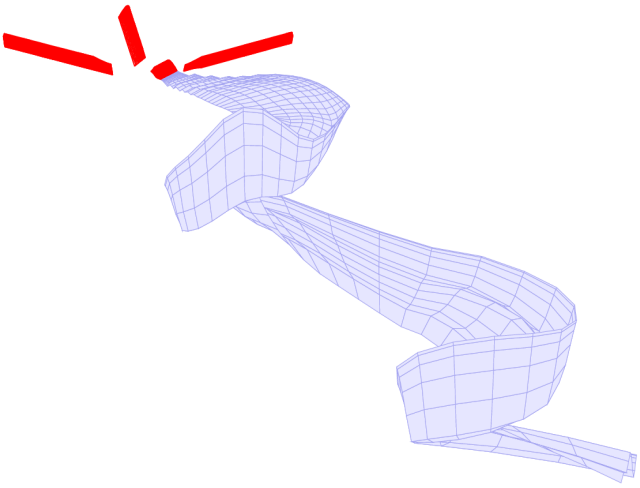

Figure 4. Deformed wake

Two different prescribed wakes have been used in the BEM solver applied for the evaluation of the perturbation responses. One is that depicted in Fig. 3 which is defined as the (undeformed) surface swept by the blade trailing edge during its motion (only one blade wake is depicted, for the sake of clarity), while the second (deformed) one is illustrated in Fig. 4 and has been obtained through the free wake BEM solver at the rotor trim condition. This approach is motivated by the significant computational time saving that is obtained with respect to that required by perturbation analysis performed using a free wake algorithm. However it is expected that the wake deformation due to the small perturbations applied in the identification of the transfer functions would yield negligible effects.

Transfer functions

Now, some of the transfer functions appearing in matrix **E** for the problem under examination are shown. Considering the flight condition corresponding to advance ratio $\mu = 0.2028$, Figs. 5 and 6 depict, respectively, real and imaginary parts of the transfer functions between the collective generalized first flap force and each multiblade perturbation. These figures show a regular behavior of these transfer functions and a very satisfactory approximation through the rational form applied (see Eq. (1)). These comments remain valid for the rest of the transfer functions not presented here, and also for those determined by the deformed prescribed wake.

The effects of the two different wake shapes consid-

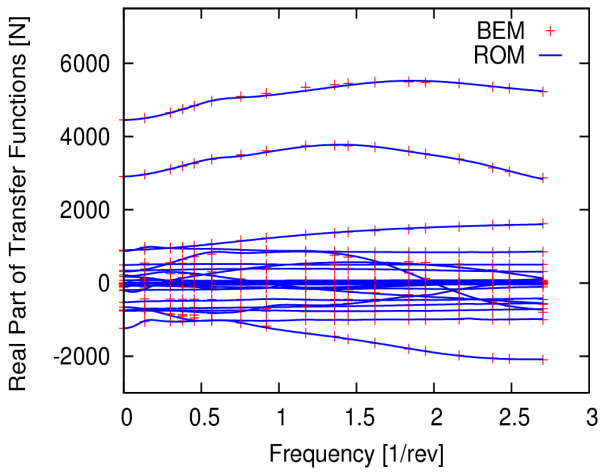

Figure 5. Real part of collective first flap force transfer functions

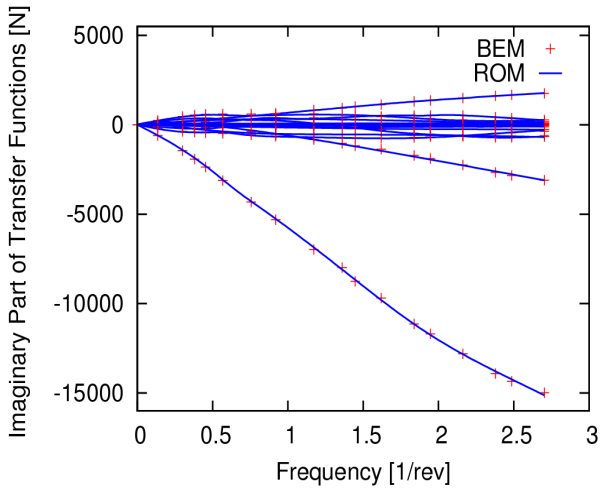

Figure 6. Imaginary part of collective first flap force transfer functions

ered on the transfer function relating collective first flap perturbation to collective generalized first flap force are depicted in Figs. 7 and 8. More appreciable differences appear between the predicted real parts of the trasfer function, but for the case examined the influence of the wake distortion is not crucial and the overall behavior is very similar.

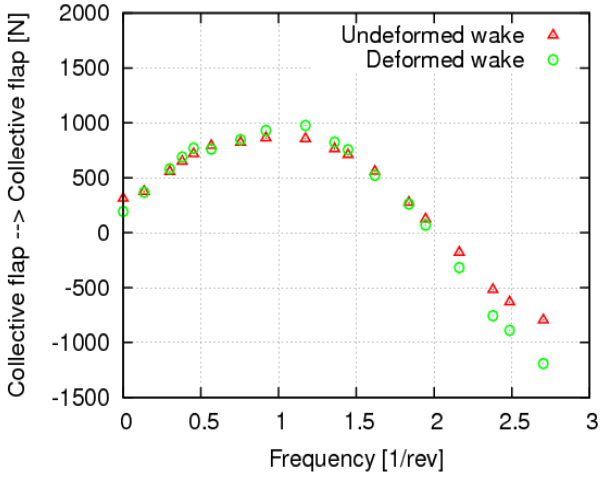

Figure 7. Real part of the transfer function between the collective first flap perturbation and collective first flap force. Undeformed vs. deformed wake.

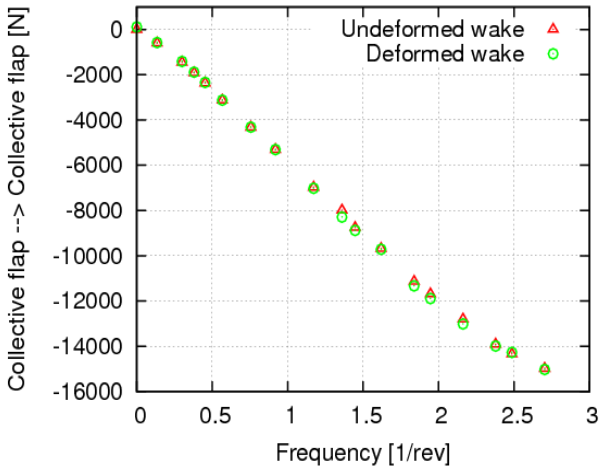

Figure 8. Imaginary part of the transfer function between the collective firts flap perturbation and collective first flap force. Undeformed vs. deformed wake.

Stability analysis

Next, the aeroelastic state-space form derived in this work has been applied to examine the aeroelastic stability of the model rotor considered. Aeroelastic dampings and frequencies have been determined through a standard eigenanalysis of the system in the form of Eq. (5). For $\mu = 0.2028$, the rotor aeroelastic eigenvalues of the first lag, flap and torsion modes, given by the ROMs based on undeformed and deformed wake shapes, as well as those given by the quasi-steady aerodynamics with static inflow are depicted in Fig. 9. It shows that the frequencies predicted by the two models are slightly different, while flap and torsion mode dampings are significantly dependent on the aerodynamic solver applied. The wake shape affects the flap and torsion scissor eigenvalues, as well as the torsion low-frequency cyclic mode. A zoom of the lag eigenvalues is depicted in Fig. 10: dampings evaluated through the ROM-BEM solver are higher than those obtained from the strip-theory approach combined with the static inflow. This means that from the point of view of the stability analysis, the simpler aerodynamic model yields conserva-

tive aeroelastic predictions. It is worth noting that in analysing phenomena where a crucial role is played by the coupling between flap rotor modes and airframe (as in rotorcraft-pilot coupling problems, for instance) the differences appearing in Fig. 10 imply that the different aerodynamic solvers considered could give considerably different aeroelastic predictions.

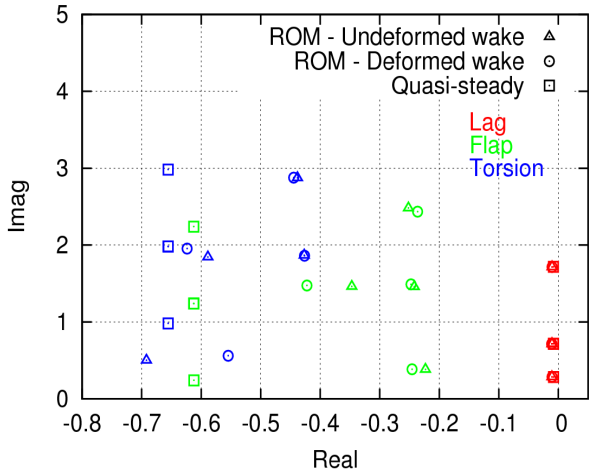

Figure 9. First lag, torsion and flap aeroelastic eigenvalues. $\mu = 0.2028$**.**

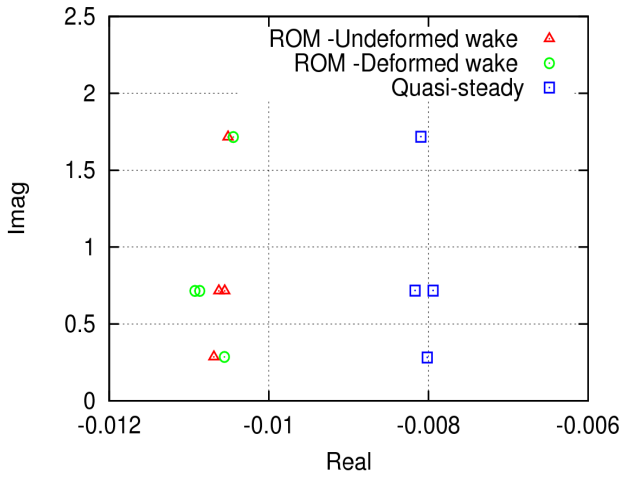

Figure 10. First lag aeroelastic eigenvalues. $\mu = 0.2028$**.**

Next the critical lag dampings for $0.04 \leq \mu \leq 0.2537$ obtained from measurements [13], from dynamic wake inflow model [13] and from the aeroelastic state-space models presented here are compared in Fig. 11. The present BEM-ROM model predicts critical dampings that are quite close to those determined experimentally, with a level of accuracy that is comparable to that observed for the simulations based on the dynamic inflow modelling [13]. According to Fig. 10 the differences between the damping predictions based on the undeformed and the deformed wake shapes are quite small. The results from the quasi-steady aerodynamic model with static inflow shows significant underprediction of the critical dampings. The differences between these results and those from the BEM-ROM solver highlight the importance of including the influence of the unsteady wake vorticity in the aeroelastic stability analysis.

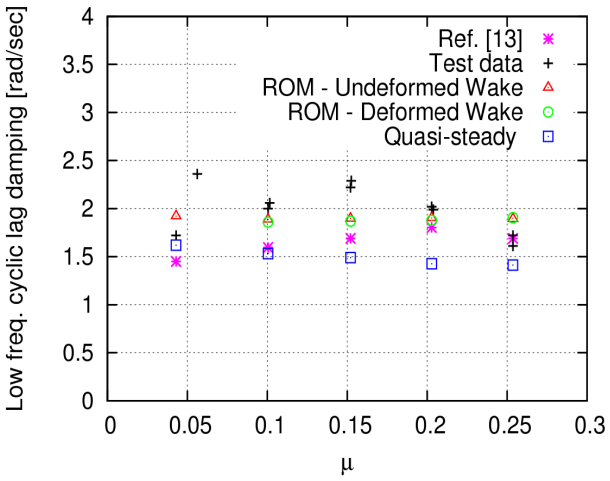

Figure 11. Low-frequency cyclic lag dampings.

The present approach seems to be unable to capture the decrease of critical damping occurring at higher values of the advance ratio. Enhanced aeroelastic stability analyses could be obtained by introducing in the solution process the rotor steady equilibrium deformations determined from the BEM solver, to replace the present ones (predicted by the simpler quasi-steady aerodynamic model).

Conclusions

A reduced-order aerodynamic model suited for deriving the state-space aeroelastic equations of helicopter rotors in arbitrary steady flight has been applied to a four bladed hingeless, soft-inplane helicopter main rotor in forward flight. This methodology is applicable to aeroelastic systems expressed in terms of multiblade coordinates, under the constant-coefficient approximation (typically acceptable at low- and mid-advance-ratio flights of rotors having more than two blades). The state-space rotor aeroelastic model has been obtained from the application of the ROM as derived from a potential aerodynamic BEM solver. The effect of the wake shape used in the aerodynamic solver (undeformed and deformed from free-wake analysis of the steady equilibrium configuration) has been investigated. This analysis shows that for the cases examined its influence is not considerable in terms of critical dampings predictions, but might become important in the analysis of phenomena where strong coupling between rotor and airframe arises. The comparisons with experimental data and dynamic wake inflow results available in the literature demonstrate that the presented ROM-BEM solver critical lag damping predictions are satisfactorily accurate. However, the slight decrease of critical dampings occurring at higher values of the advance ratio is not captured. Future enhancement of the aeroelastic solver may be obtained by considering in the stability analysis procedure rotor steady equilibrium deformations predicted by a solver based on the BEM aerodynamics.

Acknowledgments

This work has been partially supported by the European Union Project ARISTOTEL (Grant agreement N. 266073), financed under the Seventh Framework Programme (FP7/2007-2013).

References

1. Gennaretti, M., Muro, D., 'A multiblade aerodynamic reduced-order model for aeroleastic analysis of helicopter rotors in forward flight,' 36th European Rotorcraft Forum, Paris, France, Sept. 2010.
2. Peters, D.A., 'How dynamic inflow survives in the competitive world of Rotorcraft aerodynamics,' *J. of the American Helicopter Society*, Vol. 54, 2009, pp. 1-15.
3. Gaonkar, G.H., Peters, D.A., 'Review of Dynamic Inflow Modeling for Rotorcraft Flight Dynamics,' *Vertica*, Vol. 12, No. 3, 1988, pp. 213-242.
4. Peters, D.A., He, C.J., 'Finite-State Induced Flow Models, Part II: Three-Dimensional Rotor Disk,' *Journal of Aircraft,* Vol. 32, No. 2, 1995, pp. 323-333.
5. Zhao, J., 'Dynamic Wake Distortion Model for Helicopter Maneuvering Flight,' PhD Thesis, School of Aerospace Engineering, Georgia Institute of Technology, 2005.
6. Zhao, J., Prasad, J.V.R., Peters, D.A., 'Effect of Rotor Wake Distortion on the Stability of Flapping Dynamics,' American Helicopter Society 61th Annual Forum, Grapevine, TX, 2005.
7. Gennaretti, M., Greco, L., 'A Time-Dependent Coefficient Reduced-Order Model for Unsteady Aerodynamics of Proprotors,' *Journal of Aircraft,* Vol. 42, No. 1, 2005, pp. 138-147.
8. Vepa, R., 'On the Use of Padè Approximants to Represent Unsteady Aerodynamic Loads for Arbitrary Small Motions of Wings,' AIAA Guidance and Control Conference, New York, AIAA Paper 76-17, 1976.
9. Edwards, J.W., 'Application of Laplace Transform Methods to Airfoil Motion and Stability Calculations,' 20th Structures, Structural Dynamics, and Materials Conference, St. Louis, MO, AIAA Paper 79-0772, 1979.
10. Roger, K.L., 'Airplane Math Modeling Methods for Active Control Design,' AGARD-CP 228, 1977.
11. Karpel, M., 'Design for the Active Flutter Suppression and Gust Alleviation Using State-Space Aeroelastic Modeling,' *Journal of Aircraft*, Vol. 19, 1982, pp. 221-227.
12. Maier, T.H., Sharpe, D.L., Lim, J.W., 'Fundamental Investigation of Hingeless Rotor Aeroelastic Stability, Test Data and Correlation,' *American Helicopter Society 51st Annual Forum Proceedings*, Forth Worth, TX, 1995, pp. 106-117.
13. Subramanian, S., Ma, G., Gaonkar, G.H., Maier, T.H., 'Correlation of Several aerodynamic models and measurements of hingeless-rotor trim and stability,' *J. of the American Helicopter Society*, Vol. 45, 2000, pp. 106-117.
14. Hodges, D.H., Dowell, E.H., 'Nonlinear Equation for the Elastic Bending and Torsion of Twisted nonuniform Rotor Blades,' NASA TN D-7818, December 1974.
15. Gennaretti, M., Bernardini, G., 'Aeroelastic Response of Helicopter Rotors Using a 3-D Unsteady Aerodynamic Solver,' *The Aeronautical Journal*, Vol. 110, No. 1114, 2006, pp. 793-801.
16. Johnson, W., Helicopter Theory, Dover Ed., 1994.
17. Gaonkar, G.H., Peters, D.A., 'Use of Multiblade Coordinates for Helicopter Flap-Lag Stability with Dynamic Inflow,' *Journal of Aircraft,* Vol. 17, No. 2, 1980, pp. 112-118.
18. Ranjith, M., and Gaonkar, G.H., 'Unified Assessment of Fast-Floquet, Generalized Floquet, and Periodic Eigenvector Methods for Rotorcraft Stability Predictions,' Proceedings of the 66th Annual National Forum of the American Helicopter Society, Phoenix, AZ, May 2010.
19. Theodorsen, T., 'General Theory of Aerodynamic Instability and the Mechanism of Flutter,' NACA Report 496, 1935.
20. Leishman, J.G., 'Principles of Helicopter Aerodynamics,' Cambridge University Press, 2000.
21. Morino, L., Gennaretti, M., 'Boundary Integral Equation Methods for Aerodynamics,' Computational Nonlinear Mechanics in Aerospace Engineering, edited by S. N. Atluri, Vol. 146, Progress in Aeronautics and Astronautics, AIAA, Washington, D.C., 1992, pp. 279-320.
22. Hodges, D.H., Ormiston R.A., 'Stability of Elastic Bending and Torsion of Uniform Cantilever Rotor Blades in Hover with Variable Structural Coupling', NASA TN D-8192, 1976.